This is an open access article published under an ACS AuthorChoice License, which permits copying and redistribution of the article or any adaptations for non-commercial purposes.

THE JOURNAL OF PHYSICAL CHEMISTRY Letters

Letter

pubs.acs.org/JPCL

Probing the Microenvironment in the Confined Pores of Mesoporous Silica Nanoparticles

Min Xue and Jeffrey I. Zink*

Department of Chemistry and Biochemistry, University of California, Los Angeles, California 90095, United States

Supporting Information

ABSTRACT: The microenvironment inside of the pores of mesoporous silica nanoparticles is probed using spectroscopic techniques. The probe molecules are sealed inside of the pores by a nanovalve system that is capable of controlling the access to the pore and ensuring the exclusive probing of the pore environment without any interference from the probe molecules on the outer surface of the particles or from the surrounding solution. Rigidochromism studies are used to evaluate the rigidity of the solvent matrix inside of the pore, and dynamic fluorescence anisotropy experiments are employed to determine the rotational diffusion freedom of the probe molecule. The data show that those probe molecules are neither completely free to move nor tightly attached to the pore wall, and their mobility is changed by altering the charge of the pore wall.

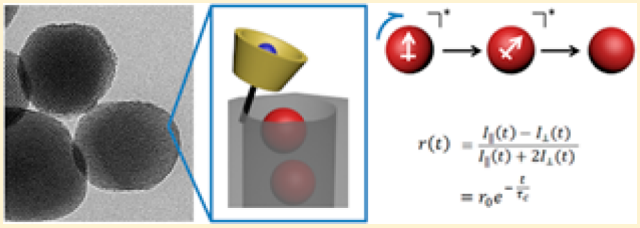

SECTION: Surfaces, Interfaces, Porous Materials, and Catalysis

The use of molecular probes and spectroscopic methods to reveal the properties of the confined environment in sol–gel films and monoliths has been well-developed.[1−15] Despite the success of those studies, little is known about the microenvironments of mesopores in silica nanoparticles. Mesoporous silica nanoparticles (MSNs) have been widely used in the field of controlled delivery, and many studies have been devoted to modifying the pore walls to accommodate the loading and docking of guest molecules.[16−19] Yet, there is limited quantitative understanding of the influences of the pore confinement on the guest molecules in these systems. It becomes more interesting when the sizes of those guest molecules are comparable to the diameter of the pore wall, where the interactions among the pore wall, the solvent molecules inside of the pore, and the guest molecules are strongly coupled. One of the major obstacles for implementing spectroscopic methods to study the interior pores of MSNs is the necessity to fully differentiate the inner surface of the pore walls versus the outer surface of the particles. In this Letter, we employ a nanovalve system[19,20] to facilitate the discrimination of the pore spaces in MSNs. Probe molecules are loaded and trapped in the mesopores by the nanovalve, while those absorbed on the outer surface are removed during subsequent washing steps. Two types of spectroscopic experiments are conducted to probe the microenvironment inside of the pores of MSNs. The rigidochromism effect provides information about the local rigidity surrounding the guest molecule,[21−24] and the dynamic fluorescence anisotropy study reveals the tumbling mobility of the guest molecule.[25−29] With these techniques, we elucidate the pore confinement effect on the guest molecules.

The MSNs are synthesized according to a well-established procedure,[16,19] and the particle size is around 100 nm while the pore diameter is around 2.3 nm (Figure 1A and the Supporting Information). A nanovalve system was grafted at the pore opening of the MSNs, which allowed us to probe primarily the mesopores with minimal interference from probe molecules either on the outer surface or in the surrounding solution.[20] This nanovalve consists of two parts, an aromatic amino compound (the "stalk") attached at the surface of the MSNs and a cyclodextrin molecule that encircles the stalk molecule via supramolecular interactions in aqueous solution (Figure 1B). The probe molecules are loaded into the pores of thread-modified MSNs, and the cyclodextrin is then introduced to form the supramolecular structure and block the pore access. After extensive washing, only those probe molecules inside of the mesopores remain for the spectroscopic studies. On the basis of TGA data and model calculations, the average number of the stalk molecules around one pore opening is estimated to be around 3.7, which is sufficient to fully control the pore access (Supporting Information). It is worth noting that the length of the pore is much greater than its diameter, and therefore, the number of the probe molecules that are in vicinity of the nanovalves makes up a negligible portion of the total probe population, ensuring minimal interference from the nanovalves.

Many guest molecules of interest, such as chemotherapy drugs that are loaded into MSNs, are hydrophilic and have diameters around 1.0−1.5 nm.[16,18,19] Therefore, a probe

Received: December 21, 2013
Accepted: February 11, 2014
Published: February 17, 2014

 © 2014 American Chemical Society

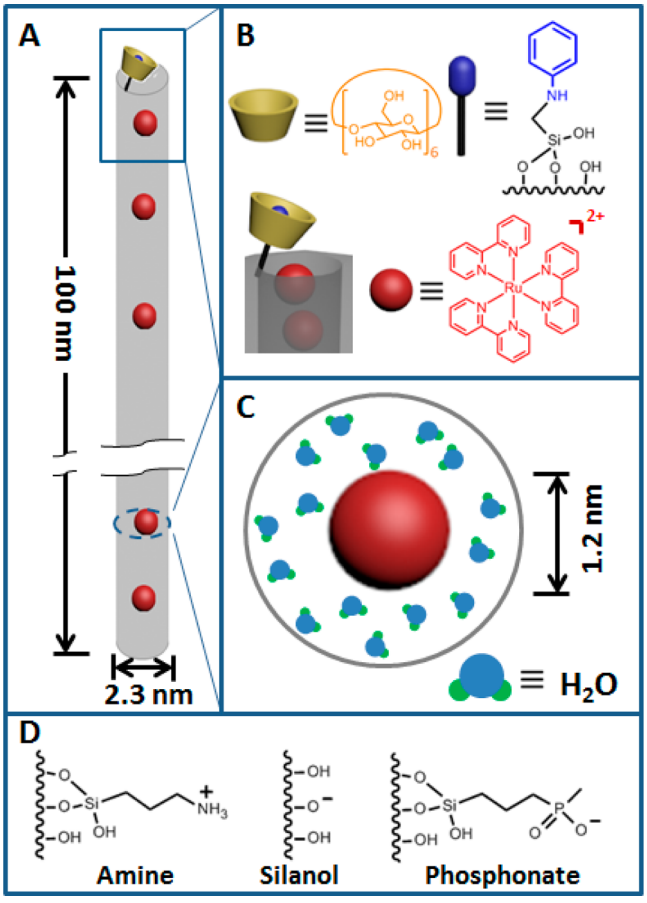

Figure 1. (A) An illustration of the probe molecules sealed inside of the mesopores by the nanovalve. (B) The components of the nanovalve. (C) A dissection of the pore showing the to-scale comparison of the sizes of the probe molecule, the pore diameter, and the water molecules. (D). Different pore wall modifications employed in this study.

molecule is chosen to have similar properties. Once they are loaded into the pores, the space between the guest molecule and the pore wall fits at most three to four water molecules (Figure 1C). This leads to a complicated interaction between the guest molecule and the pore wall that cannot be treated as either a "molecule in solvent" or a "molecule on substrate" model. In order to minimize preferential orientation of long aspect molecules along the pore direction, the probe molecule needs to be highly symmetric to average out the potentially anisotropic influence from the pore wall and the solvent molecules inside of the pore. Moreover, the fluorescence lifetime of the probe needs to be long enough to allow an ample time window for the spectroscopic studies. With those criteria, tris(bipyridine)ruthenium(II)hexafluorophosphate (RuBPy) was chosen as the probe due to its appropriate size, water solubility, highly symmetric shape (D_3 point group), and long fluorescence lifetime. Around 0.8 wt % of RuBPy was loaded into the nanoparticles, and the average distance between two RuBPy molecules inside of the pore was estimated to be around 11 nm (Supporting Information), which is long enough to prevent interference from intermolecular energy transfer among the RuBPy molecules.

Different pore environments are achieved by modifying the pore walls with either 3-aminopropyltriethoxysilane or 3-(trihydroxysilyl)propylmethylphosphonate to introduce positive or negative charges, respectively. These charge modifications inside of the mesopores help evaluate the behavior of probe molecules inside of the confined mesopores (Figure 1D).

Rigidochromism studies provide a simplified picture about the rigidity of the environment inside of the pore. The principle of the rigidochromic effect is illustrated in Figure 2. Generally,

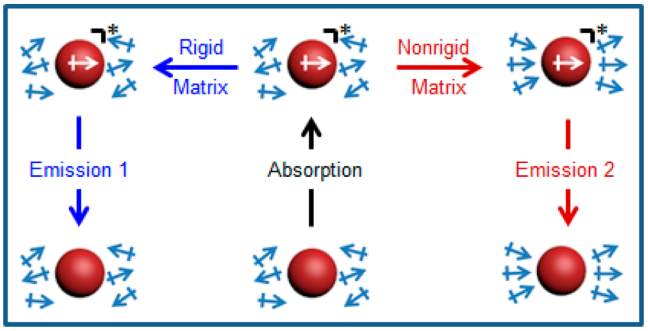

Figure 2. The principle of the rigidochromism effect. The energy of emission 1 is higher than that of emission 2 due to the inability of the matrix molecule reorientation. The corresponding Stokes shift for emission 1 is smaller than that of emission 2.

when a RuBPy molecule is placed in a solvent matrix, the surrounding solvent dipole moments can be considered to be randomly oriented because its ground-state permanent dipole moment is negligible.[30−32] When the RuBPy is in its metal-to-ligand charge-transfer excited state, it has a relatively large dipole moment with a direction from a ligand to the metal center.[32,33] If the solvent molecules are free to move, they reorient themselves such that their dipole moments align with that of the excited RuBPy molecule. In this case, the emission from the RuBPy molecule has a relatively lower energy. On the contrary, when the surrounding environment is rigid, the solvent molecules will not reorient, and the corresponding emission from this RuBPy molecule is at a higher energy.[3,9]

The absorption and emission maxima of different samples are summarized in Table 1. When loaded into the confined

Table 1. Results Summary of the Rigidochromism Studies

	wavenumber (cm^{-1}) × 10^3		
samples	absorption	emission	Stokes shift
RuBPy solution	22.08	16.26	5.82
amine	21.88	16.32	5.56
silanol	21.88	16.50	5.38
phosphonate	21.88	16.63	5.25

mesopores, the Stokes shift of RuBPy decreases compared to that of the RuBPy solution. This result indicates that the water molecules inside of the mesopores are less mobile than those in a bulk solution and form a more rigid matrix. The positively charged amine-modified sample gives a Stokes shift of 5.56 × 10^3 cm^{-1}, which has a lower energy than that of the negatively charged samples (the phosphonated sample at 5.25 × 10^3 cm^{-1} and the silanol−surface sample at 5.38 × 10^3 cm^{-1}). This result shows that the RuBPy molecules are in a more rigid environment as the surrounding pore wall becomes more negatively charged. When the pore wall becomes more negatively charged, the RuBPy molecules are more strongly attached to the pore wall. This change accounts for the increased rigidity of the local environment because the water

dx.doi.org/10.1021/jz402760b | J. Phys. Chem. Lett. 2014, 5, 839−842

molecules close to the pore wall are more rigid than those in the middle of the pore, and the effect of the rigid silica wall on the RuBPy becomes more prominent.

In order to achieve a more detailed understanding of the pore confinement effect posed on the guest molecule, dynamic fluorescence anisotropy experiments are employed to evaluate the tumbling freedom of the RuBPy molecule. In these experiments, RuBPy molecules encapsulated in the mesopores are irradiated by a polarized excitation pulse beam, and the fluorescence anisotropy of the emitted light is measured. Because the probability of exciting a fluorophore molecule depends on the angle between the transition dipole and the electric field vector of the excitation light and because the fluorophore molecules are randomly oriented, the resulting fluorescence emission is partially polarized, and this can be characterized by the fluorescence anisotropy (Figure 3A).

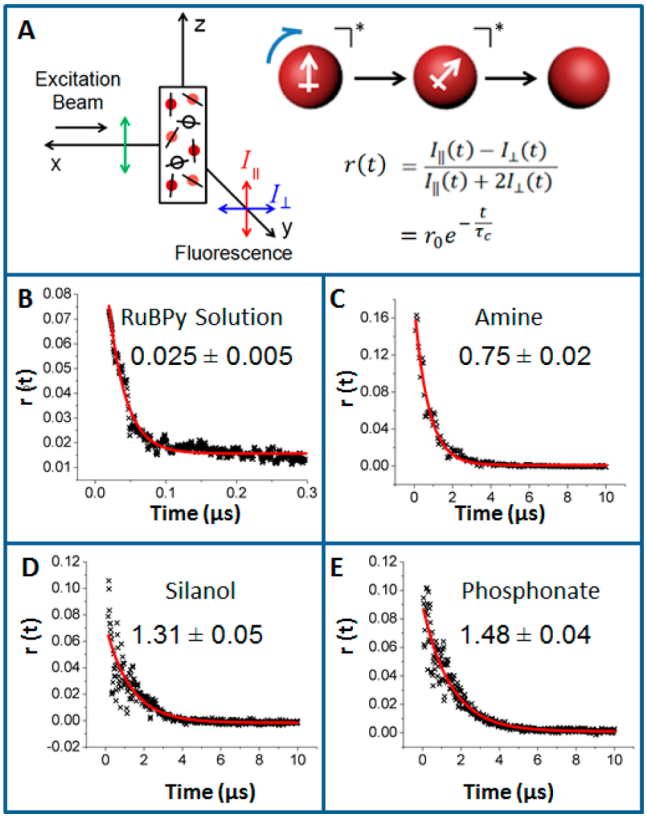

Figure 3. (A) The principle of the dynamic fluorescence anisotropy studies. (B–E) The fluorescence anisotropy data for different samples (black crosses), the fitted curve for the exponential anisotropy decay (red curves), and the calculated fluorescence anisotropy correlation time τ_c for each sample.

When the molecules are mobile in the environment, the tumbling of the excited molecules before their emission causes a decay of the fluorescence anisotropy. This decay can be continuously monitored, and the corresponding curve can be fitted with a single-exponential function. The decay time constant, which is defined as the fluorescence anisotropy correlation time τ_c, reflects the rate of the rotational diffusion of the RuBPy molecule and therefore reveals the pore confinement effect on the molecule.[27,29]

The fitting of the fluorescence anisotropy decay curves is shown in Figure 3B. The τ_c values obtained from the fitting are listed for each sample. Meanwhile, the fluorescence lifetime of each sample is also calculated through fitting the total fluorescence intensity decay with an exponential decay curve (Supporting Information). The amine-modified, positively charged sample gave a fluorescence correlation time of 0.75 μs and a fluorescence lifetime of 1.15 μs. This lifetime is much longer than that of a RuBPy solution (0.49 μs) and is indicative of the entrapment of RuBPy inside of the pores. The fluorescence correlation time (0.75 μs) is also an order of magnitude longer than that of the RuBPy solution (0.025 μs), which proves that the RuBPy molecules are in a restrained environment and their mobility is highly limited.

The emission lifetimes in the phosphonated and the silanol samples are 0.84 and 0.94 μs, respectively, which are similar to each other but different from the values from the solution and the amine-modified samples. This indicates that the RuBPy molecules are in a different environment and is caused by the negatively charged pore surfaces in the phosphonated and the silanol-surfaced samples. The silanol–surface sample exhibited a fluorescence correlation time of 1.31 μs, and the phosphonated sample gave 1.48 μs. These values are much larger than that of the anime-modified sample, which reveals that Ru-triBPy molecules are much less mobile in these negatively charged environments than in a positively charged one. This result is expected because the RuBPy ion is positively charged and the charge distribution is symmetric. In the negatively charged samples, the Ru-triBPy molecules are most likely more attached onto the pore wall because of the electrostatic attraction, which significantly decreases their mobility. In contrast, the positively charged wall in the amine-modified sample does not have strong affinity toward RuBPy cations. As a result, the RuBPy molecules can move more freely. This result is consistent with that from the rigidochromism studies, where the positively charged wall appears to have less impact on the environment rigidity surrounding the RuBPy molecules.

In summary, nanovalves facilitate the study of the properties inside of confined mesopores of MSNs and help eliminate the interferences from the outer surface and the surrounding solution. When the size of the guest molecules is comparable with the pore diameter, the effect of the pore wall confinement is prominent, and this can be quantitatively determined and compared among different pore wall modifications by using rigidochromism and dynamic fluorescence anisotropy studies. Our data prove that these guest molecules are neither completely free to move nor tightly attached to the pore wall, and their mobility can be strongly affected by the charge modification of the pore wall.

■ ASSOCIATED CONTENT

Ⓢ Supporting Information

The synthesis and characterizations of MSNs, the spectroscopic experimental setup and the data processing procedure, the absorption and fluorescence spectra of different samples in the rigidochromism studies, the fluorescence intensity curves, and the fittings for the fluorescence lifetimes of each sample. This material is available free of charge via the Internet at http://pubs.acs.org.

■ AUTHOR INFORMATION

Corresponding Author

*E-mail: zink@chem.ucla.edu.

dx.doi.org/10.1021/jz402760b | J. Phys. Chem. Lett. 2014, 5, 839–842

Notes

The authors declare no competing financial interest.

■ ACKNOWLEDGMENTS

This work is supported by NIH CA133697 and USDOD-HDTRA1-13-1-0046. The authors would like to thank Dr. Zongxi Li and Dr. Bryana Henderson for helpful discussions.

■ REFERENCES

(1) Gvishi, R.; Narang, U.; Bright, F. V.; Prasad, P. N. Probing the Microenvironment of Polymer-Impregnated Composite Glass Using Solvatochromic Dye. *Chem. Mater.* **1995**, *7*, 1703−1708.
(2) Narang, U.; Bright, F. V. Conformational Flexibility of 1,3-Bis(1-pyrenyl)propane throughout the Sol−Gel to Xerogel Process. *Chem. Mater.* **1996**, *8*, 1410−1414.
(3) Dunn, B.; Zink, J. I. Probes of Pore Environment and Molecule−Matrix Interaction in Sol−Gel Materials. *Chem. Mater.* **1997**, *9*, 2280−2291.
(4) Huang, M. H.; Dunn, B. S.; Zink, J. I. In Situ Luminescence Probing of the Chemical and Structural Changes during Formation of Dip-Coated Lamellar Phase Sodium Dodecyl Sulfate Sol−Gel Thin Films. *J. Am. Chem. Soc.* **2000**, *122*, 3739−3745.
(5) Keeling-Tucker, T.; Brennan, J. D. Fluorescent Probes as Reporters on the Local Structure and Dynamics in Sol−Gel-Derived Nanocomposite Materials. *Chem. Mater.* **2001**, *13*, 3331−3350.
(6) Viteri, C. R.; Gilliland, J. W.; Yip, W. T. Probing the Dynamic Guest−Host Interactions in Sol−Gel Films Using Single Molecule Spectroscopy. *J. Am. Chem. Soc.* **2003**, *125*, 1980−1987.
(7) Pagliaro, M.; Ciriminna, R.; Man, M. W. C.; Campestrini, S. Better Chemistry through Ceramics: The Physical Bases of the Outstanding Chemistry of ORMOSIL. *J. Phys. Chem. B* **2006**, *110*, 1976−1988.
(8) Yamaguchi, A.; Amino, Y.; Shima, K.; Suzuki, S.; Yamashita, T.; Teramae, N. Local Environments of Coumarin Dyes within Mesostructured Silica−Surfactant Nanocomposites. *J. Phys. Chem. B* **2006**, *110*, 3910−3916.
(9) Dunn, B. S.; Zink, J. I. Molecules in Glass: Probes, Ordered Assemblies, and Functional Materials. *Acc. Chem. Res.* **2007**, *40*, 747−755.
(10) Jung, C.; Hellriegel, C.; Platschek, B.; Wöhrle, D.; Bein, T.; Michaelis, J. Bräuchle Simultaneous Measurement of Orientational and Spectral Dynamics of Single Molecules in Nanostructured Host−Guest Materials. *J. Am. Chem. Soc.* **2007**, *129*, 5570−5579.
(11) Malfatti, L.; Kidchob, T.; Aiello, D.; Aiello, R.; Testa, F.; Innocenzi, P. Aggregation States of Rhodamine 6G in Mesostructured Silica Films. *J. Phys. Chem. C* **2008**, *112*, 16225−16230.
(12) Rei, A.; Hungerford, G.; Ferreira, M. I. C. Probing Local Effects in Silica Sol−Gel Media by Fluorescence Spectroscopy of p-DASPMI. *J. Phys. Chem. B* **2008**, *112*, 8832−8839.
(13) Lei, Q.; Yip, W. T. Probing the Effect of Post-Synthesis Grafting on Guest−Host Interactions in Sol−Gel Silica with Single-Molecule Mobility and Photostability. *J. Phys. Chem. C* **2009**, *113*, 21130−21138.
(14) Pardo, R.; Zayat, M.; Levy, D. Photochromic Organic−Inorganic Hybrid Materials. *Chem. Soc. Rev.* **2011**, *40*, 672−687.
(15) Ciriminna, R.; Sciortino, M.; Alonzo, G.; de Schrijver, A.; Pagliaro, M. From Molecules to Systems: Sol−Gel Microencapsulation in Silica-Based Materials. *Chem. Rev.* **2011**, *111*, 765−789.
(16) Trewyn, B. G.; Slowing, I. I.; Giri, S.; Chen, H.-T.; Lin, V. S.-Y. Synthesis and Functionalization of a Mesoporous Silica Nanoparticle Based on the Sol−Gel Process and Applications in Controlled Release. *Acc. Chem. Res.* **2007**, *40*, 846−853.
(17) Schlossbauer, A.; Warncke, S.; Gramlich, P. M. E.; Kecht, J.; Manetto, A.; Carell, T.; Bein, T. A Programmable DNA-Based Molecular Valve for Colloidal Mesoporous Silica. *Angew. Chem., Int. Ed.* **2010**, *49*, 4734−4737.
(18) Tang, F.; Li, L.; Chen, D. Mesoporous Silica Nanoparticles: Synthesis, Biocompatibility and Drug Delivery. *Adv. Mater.* **2012**, *24*, 1504−1534.
(19) Li, Z.; Barnes, J. C.; Bosoy, A.; Stoddart, J. F.; Zink, J. I. Mesoporous Silica Nanoparticles in Biomedical Applications. *Chem. Soc. Rev.* **2012**, *41*, 2590−2605.
(20) Du, L.; Liao, S.; Khatib, H. A.; Stoddart, J. F.; Zink, J. I. Controlled-Access Hollow Mechanized Silica Nanocontainers. *J. Am. Chem. Soc.* **2009**, *131*, 15136−15142.
(21) Wrighton, M.; Morse, D. L. Nature of the Lowest Excited State in Tricarbonylchloro-1,10-phenanthrolinerhenium(I) and Related Complexes. *J. Am. Chem. Soc.* **1974**, *96*, 998−1003.
(22) McKiernan, J.; Pouxviel, J. C.; Dunn, B.; Zink, J. I. Rigidochromism as a Probe of Gelation and Densification of Silicon and Mixed Aluminum−Silicon Alkoxides. *J. Phys. Chem.* **1989**, *93*, 2129−2133.
(23) Itokazu, M. K.; Polo, A. S.; Iha, N. Y. M. Luminescent Rigidochromism of Fac-$[Re(CO)_3(phen)(cis\text{-}bpe)]^+$ and Its Binuclear Complex as Photosensors. *J. Photochem. Photobiol., A* **2003**, *160*, 27−32.
(24) Rivera, E. J.; Barbosa, C.; Torres, R.; Rivera, H.; Fachini, E. R.; Green, T. W.; Connick, W. B.; Colon, J. L. Luminescence Rigidochromism and Redox Chemistry of Pyrazolate-Bridged Binuclear Platinum(II) Diimine Complex Intercalated into Zirconium Phosphate Layers. *Inorg. Chem.* **2012**, *51*, 2777−2784.
(25) Straume, M.; Litman, B. Influence of Cholesterol on Equilibrium and Dynamic Bilayer Structure of Unsaturated Acyl Chain Phosphatidylcholine Vesicles as Determined from Higher Order Analysis of Fluorescence Anisotropy Decay. *Biochemistry* **1987**, *26*, 5121−5126.
(26) L'Espérance, D.; Chronister, E. L. Rotational Dynamics of Quinizarin in Silicate and Aluminosilicate Solutions, Gels, and Glasses. *Chem. Phys. Lett.* **1993**, *201*, 229−235.
(27) Valeur, B. *Molecular Fluorescence: Principles and Applications*; Wiley-VCH: Weinheim, Germany, 2001.
(28) Clayton, A. H. A.; Hanley, Q. S.; Arndt-Jovin, D. J.; Subramaniam, V.; Jovin, T. M. Dynamic Fluorescence Anisotropy Imaging Microscopy in the Frequency Domain (rFLIM). *Biophys. J.* **2002**, *83*, 1631−1649.
(29) Lakowicz, J. R. *Principles of Fluorescence Spectroscopy*; Springer: Berlin, Germany, 2006.
(30) Bradley, P. G.; Kress, N.; Hornberger, B. A.; Dallinger, R. F.; Woodruff, W. H. Vibrational Spectroscopy of the Electronically Excited State. 5. Time-Resolved Resonance Raman Study of Tris(bipyridine)ruthenium(II) and Related Complexes. Definitive Evidence for the "Localized" MLCT State. *J. Am. Chem. Soc.* **1981**, *103*, 7441−7446.
(31) Malone, R. A.; Kelley, D. F. Interligand Electron Transfer and Transition State Dynamics in Ru(II)trisbipyridine. *J. Chem. Phys.* **1991**, *95*, 8970−8976.
(32) Kober, E. M.; Sullivan, B. P.; Meyer, T. J. Solvent Dependence of Metal-to-Ligand Charge-Transfer Transitions. Evidence for Initial Electron Localization in MLCT Excited States of 2,2′-Bipyridine Complexes of Ruthenium(II) and Osmium(II). *Inorg. Chem.* **1984**, *23*, 2098−2104.
(33) Oh, D. H.; Boxer, S. G. Stark Effect Spectra of $Ru(diimine)_3^{2+}$ Complexes. *J. Am. Chem. Soc.* **1989**, *111*, 1130−1131.